CHAPTER 4

RESULTS AND DISCUSSION

4.1 POLYMERIZATION PROCEDURE

The ring-opening polymerization of L(-)-lactide, hereafter referred to as simply L-lactide, was conducted in the bulk phase. Prior to polymerization, the purified L-lactide monomer was crushed to a fine powder and again dried under vacuum at 55 °C. For each condition, the dried monomer (approx. 8 g) was accurately weighed into a 25 ml round-bottomed flask equipped with a magnetic stirrer, together with either stannous octoate or stannous oxalate (0.02 mol %) as catalyst and diethylene glycol (0.04 mol %) as initiator. These weighings were carried out under a dry N_2 atmosphere in a glove box in order to avoid contact and possible hydrolysis of the monomer by atmospheric moisture.

The polymerization flasks were immersed in a silicone oil bath (Figure 4.1) at either 140 °C or 180 °C for various times up to 72 hrs. At the end of each polymerization time, one flask was removed from the oil bath and allowed to cool to room temperature. The polymerizate was dissolved in chloroform as solvent and the polymer precipitated from solution by dropwise addition into ice-cooled methanol, an appropriate non-solvent, as shown in Figure 4.2. The series of polymerization experiments that were carried out in this work are summarized in Table 4.1.

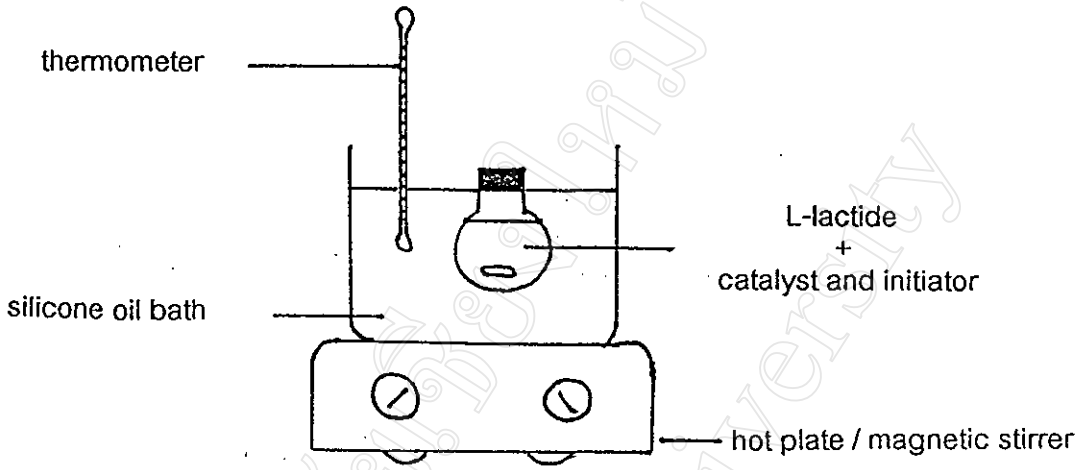

Figure 4.1 Apparatus used for the ring-opening polymerization of L-lactide.

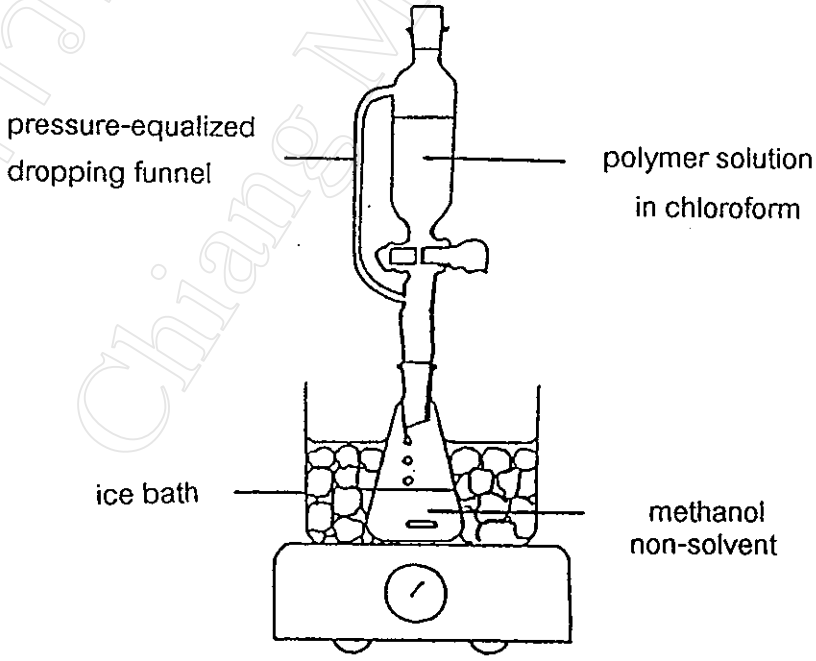

Figure 4.2 Apparatus used for the purification of the crude polymer by precipitation from solution.

Table 4.1 Summary of L-lactide polymerization conditions employed in this work.

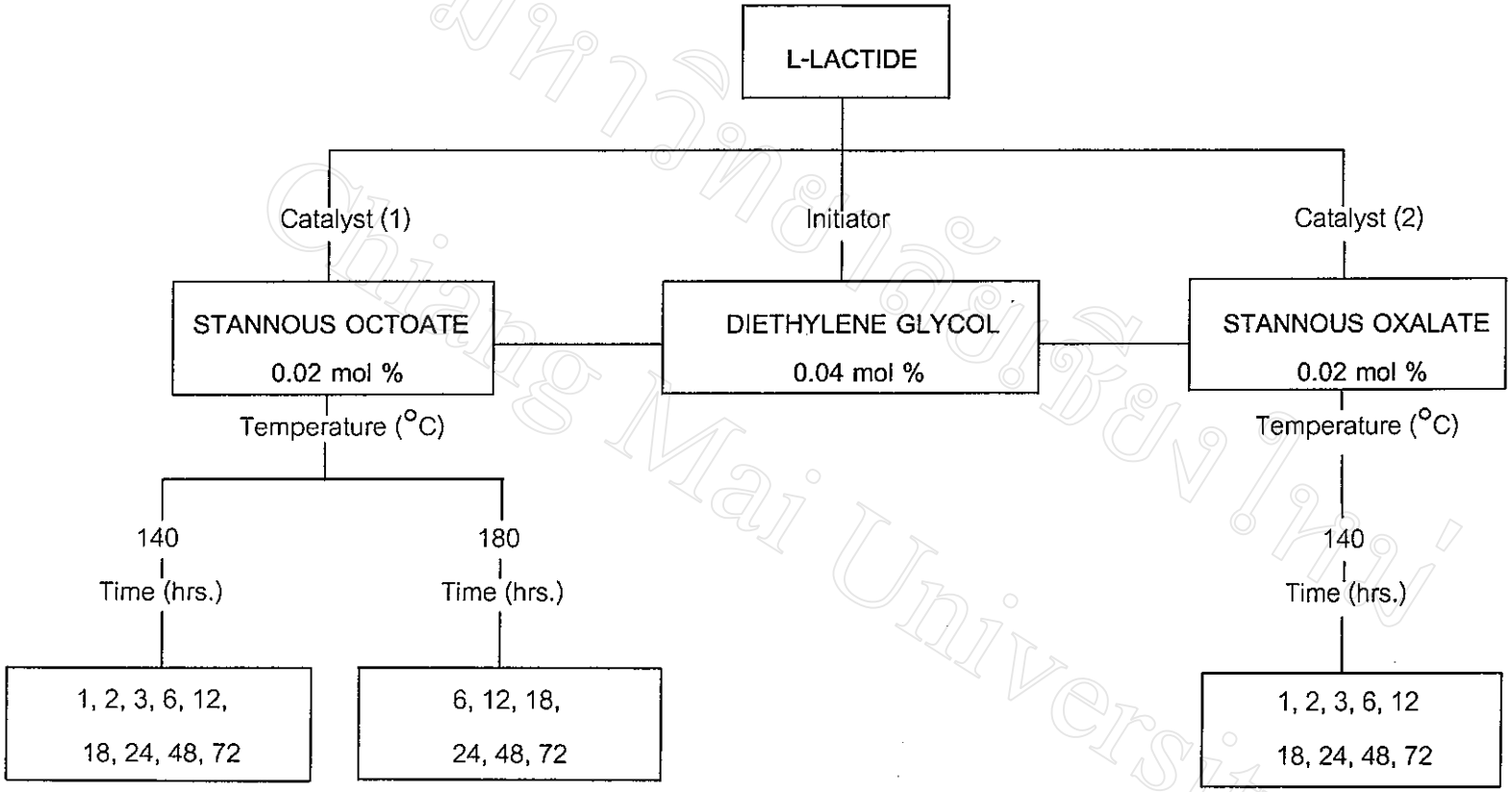

MOLE RATIO : Monomer : Initiator : Catalyst = 5000 : 2 : 1

4.2 POLYMERIZATION RESULTS

4.2.1 Polymer Yields and Average Molecular Weights

The results of the 3 polymerization experiments are given in Tables 4.3 – 4.5. The polymer yields (g) are converted into % conversions through the equation:

$$\% \text{ Conversion} = \frac{\text{Polymer Yield (g)}}{\text{Initial Wt. of Monomer (g)}} \times 100\ \%$$

Sample Calculation of % Conversion :

For the first sample (time = 1 hour) in Table 4.3

$$\% \text{ Conversion} = \frac{0.1621\ \text{g}}{8.0023\ \text{g}} \times 100\ \% = 2.03\ \%$$

The viscosity-average molecular weight ($\bar{M}_V$) values in Tables 4.3 – 4.5 were determined from dilute-solution viscometry, as previously described. An example of the type of flow-time data obtained, derived viscosity parameters, and reduced/inherent viscosity-concentration graphs are shown in Table 4.2 and Figure 4.3. The double extrapolation of the 2 graphs in Figure 4.3 to their common intercept at zero concentration (c=0) gives the value of the intrinsic viscosity, $[\eta]$, from which the value of $\bar{M}_V$ is calculated as follows:

Sample Calculation of $\bar{M}_V$:

From Figure 4.3 on the following page

$$[\eta] = (\eta_{red})_{c=o} = (\eta_{inh})_{c=o} = 1.69 \text{ dl/g}$$

When this value of $[\eta]$ is substituted into the Mark-Houwink-Sakurada Equation for poly(L-lactide) in chloroform as solvent at 25 °C [29] of :

$$[\eta] = 5.45 \times 10^{-4} \bar{M}_V^{0.73} \text{ dl/g}$$

it yields

$$1.69 = 5.45 \times 10^{-4} \bar{M}_V^{0.73}$$

from which

$$\bar{M}_V = 6.10 \times 10^4$$

The values of the % conversion and $\bar{M}_V$ in Tables 4.3 – 4.5, when considered as a function of time (hrs.), provide valuable information regarding the nature of the polymerization reaction, in particular the kinetic profiles of monomer conversion and chain growth. These kinetic profiles are compared and discussed in section 4.3.

Table 4.2 Dilute-solution viscometry data using chloroform as solvent at 25 °C for the poly(L-lactide) synthesized at 140 °C for 72 hrs. using stannous octoate as catalyst.

Concentration (g/dl)	Flow-time* (s)	η_{rel}	η_{sp}	η_{red} (dl/g)	η_{inh} (dl/g)
0	328.6	-	-	-	-
0.100	387.7	1.180	0.180	1.792	1.648
0.204	455.4	1.386	0.386	1.896	1.604
0.302	529.3	1.612	0.612	2.028	1.582
0.408	610.8	1.859	0.859	2.107	1.521

* average of at least 3 readings which agreed to within ± 0.2 % of the average value

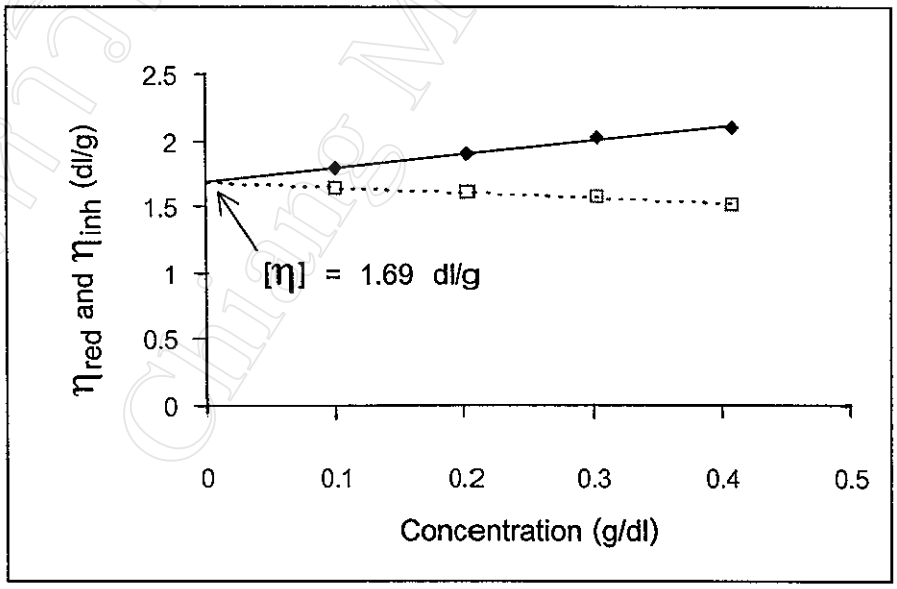

Figure 4.3 Reduced (η_{red}) and inherent (η_{inh}) viscosity-concentration plots for poly(L-lactide) synthesized at 140 °C for 72 hrs. using stannous octoate as catalyst. (♦ η_{red} and □ η_{inh})

Table 4.3 Polymerization of L-lactide at 140 °C using stannous octoate as catalyst.

L-lactide (MONOMER) (g)	Stannous octoate (CATALYST) (g)	Diethylene glycol (INITIATOR) (g)	Time (hrs.)	Physical Appearance of Purified Polymer at Room Temperature	Polymer Yield (g)	Conversion (%)	Intrinsic Viscosity** [η] (dl/g)	Viscosity-Average Mol. Wt. $\bar{M}_v$
8.0023	0.0041	0.0023	1	white powder	0.1621	2.03	-	-
8.0019	0.0043	0.0022	2	white powder	0.3623	4.53	-	-
8.0055	0.0044	0.0023	3	white granular solid	2.2796	28.48	0.53	1.24×10^4
8.0112	0.0044	0.0024	6	white granular solid	5.4273	67.75	1.05	3.20×10^4
8.0014	0.0046	0.0022	12*	white granular solid	7.4793	93.47	1.23	3.90×10^4
8.0092	0.0047	0.0022	18*	white granular solid	7.3462	91.72	1.20	3.80×10^4
8.0190	0.0048	0.0021	24*	white granular solid	7.4129	92.44	1.40	4.70×10^4
8.0145	0.0048	0.0024	48*	white granular solid	7.7976	97.29	1.34	4.40×10^4
8.0010	0.0043	0.0024	72*	white granular solid	7.7746	97.17	1.69	6.10×10^4

[Stannous octoate] = 0.02 mol % [Diethylene glycol] = 0.04 mol %

* polymerizate solidified at 140 °C ⟶ solid-state polymerization

** as measured in chloroform as solvent at 25 °C

Table 4.4 Polymerization of L-lactide at 180 °C using stannous octoate as catalyst.

L-lactide (MONOMER) (g)	Stannous octoate (CATALYST) (g)	Diethylene glycol (INITIATOR) (g)	Time (hrs.)	Physical Appearance of Purified Polymer at Room Temperature	Polymer Yield (g)	Conversion (%)	Intrinsic Viscosity** [η] dl/g	Viscosity-Average Mol. Wt. $\bar{M}_v$
8.0055	0.0048	0.0026	6*	white granular solid	7.7935	97.35	1.23	3.90×10^4
8.0104	0.0048	0.0026	12*	white granular solid	7.5444	94.18	0.95	2.75×10^4
8.0099	0.0045	0.0025	18*	white granular solid	7.8902	98.50	1.19	3.75×10^4
8.0070	0.0045	0.0024	24*	white granular solid	7.7618	96.94	1.11	3.40×10^4
8.0022	0.0048	0.0025	48*	white granular solid	7.2558	90.67	0.75	2.00×10^4

[Stannous octoate] = 0.02 mol % [Diethylene glycol] = 0.04 mol %

* polymerizate solidified at 180 °C ⟶ solid-state polymerization

** as measured in chloroform as solvent at 25 °C

Table 4.5 Polymerization of L-lactide at 140 °C using stannous oxalate as catalyst.

L-lactide (MONOMER) (g)	Stannous oxalate (CATALYST) (g)	Diethylene glycol (INITIATOR) (g)	Time (hrs.)	Physical Appearance of Product at Room Temperature	Polymer Yield (g)	Conversion (%)	Intrinsic Viscosity** [η] dl/g	Viscosity-Average Mol. Wt. $\bar{M}_v$
8.0052	0.0024	0.0025	1	-	0	0	-	-
8.0052	0.0024	0.0025	2	-	0	0	-	-
8.0041	0.0021	0.0025	3	-	0	0	-	-
8.0040	0.0025	0.0025	6	-	0	0	-	-
8.0042	0.0026	0.0023	12	white powder	0.0554	0.69	-	-
8.0030	0.0022	0.0026	18	white granular solid	2.2398	27.99	0.48	1.10×10^4
8.0027	0.0022	0.0024	24	white granular solid	1.9900	24.87	0.54	1.27×10^4
8.0074	0.0022	0.0025	48	white granular solid	4.3529	54.36	0.88	2.50×10^4
8.0376	0.0022	0.0025	72*	white granular solid	7.7061	95.88	1.29	4.20×10^4

[Stannous oxalate] = 0.02 mol % [Diethylene glycol] = 0.04 mol %

* polymerizate solidified at 140 °C ⟶ solid-state polymerization

** as measured in chloroform as solvent at 25 °C

4.2.2 Polymer Thermal Transitions

The thermal transitions of the purified polymer products were determined by differential scanning calorimetry (DSC). These transitions included the glass transition temperature (T_g), the solid-state crystallization temperature (T_c), and the crystalline melting point (T_m).

The DSC thermograms of the highest molecular weight poly(L-lactide) products from each of the 3 polymerization experiments are shown in Figures 4.4–4.6 as examples. Each curve clearly shows the glass transition, a solid-state crystallization exotherm, and a melting endotherm in order of appearance as the temperature increases. In each ease, a heating rate of 10 °C/min was used under a nitrogen atmosphere with a sample size of 3 – 5 mg. The values of T_g, T_c and T_m as well as the values of the heat of melting (ΔH_m) and % crystallinity for each sample are compared in Tables 4.6 – 4.8.

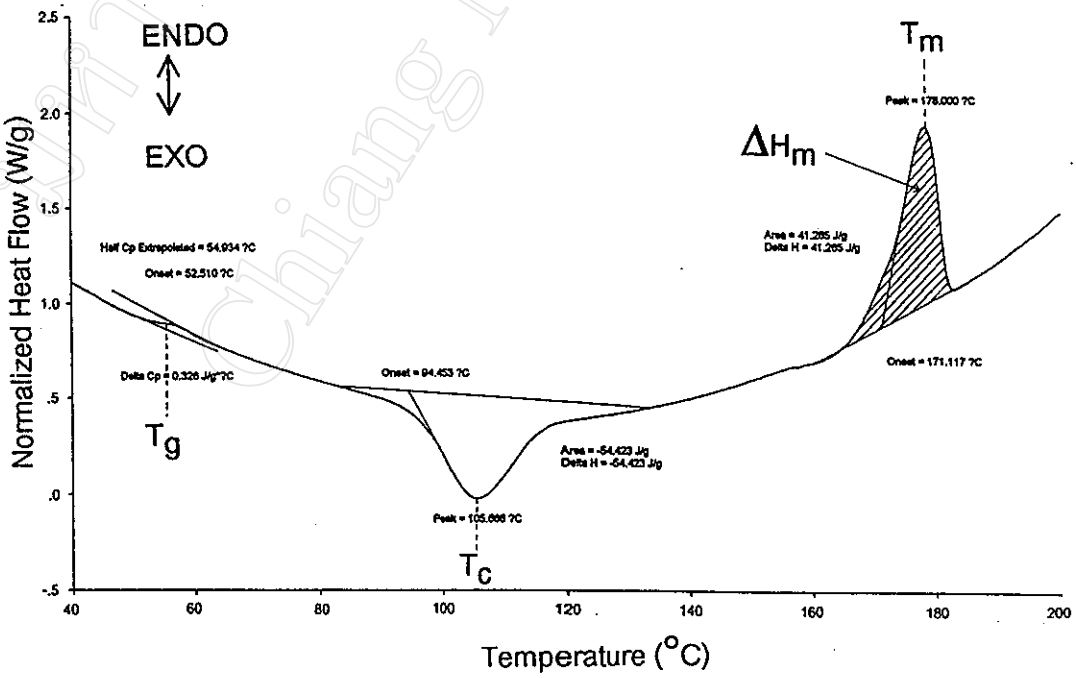

Figure 4.4 DSC thermogram of the poly(L-lactide) synthesized at 140 °C for 72 hrs using $Sn(Oct)_2$ as catalyst. (Sample size = 3.900 mg)

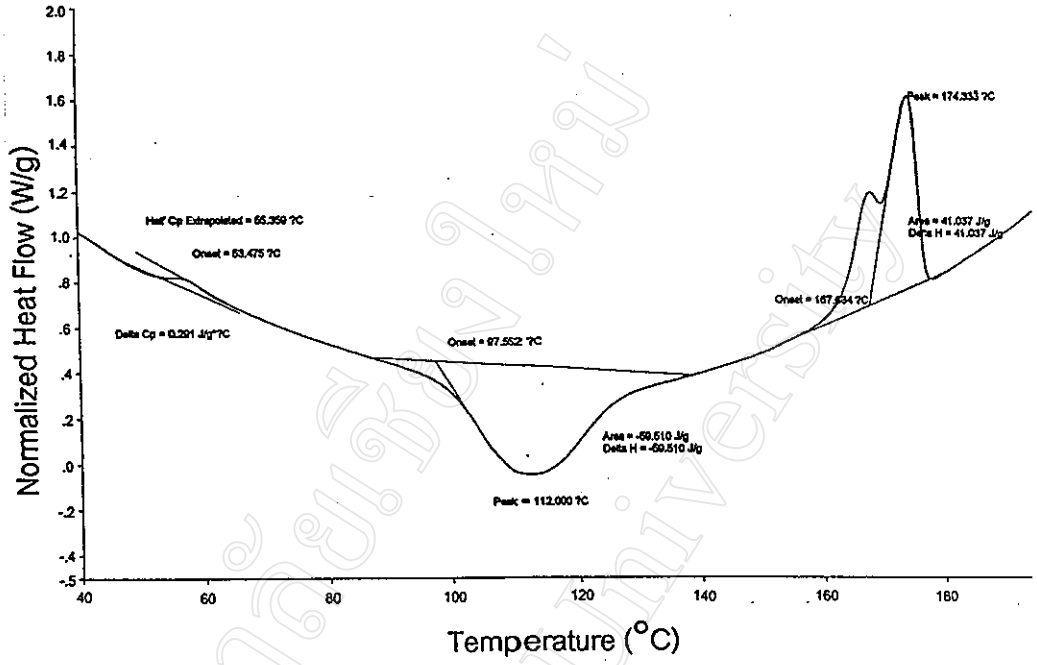

Figure 4.5 DSC thermogram of the poly(L-lactide) synthesized at 180 °C for 6 hrs using $Sn(Oct)_2$ as catalyst. (Sample size= 4.220 mg)

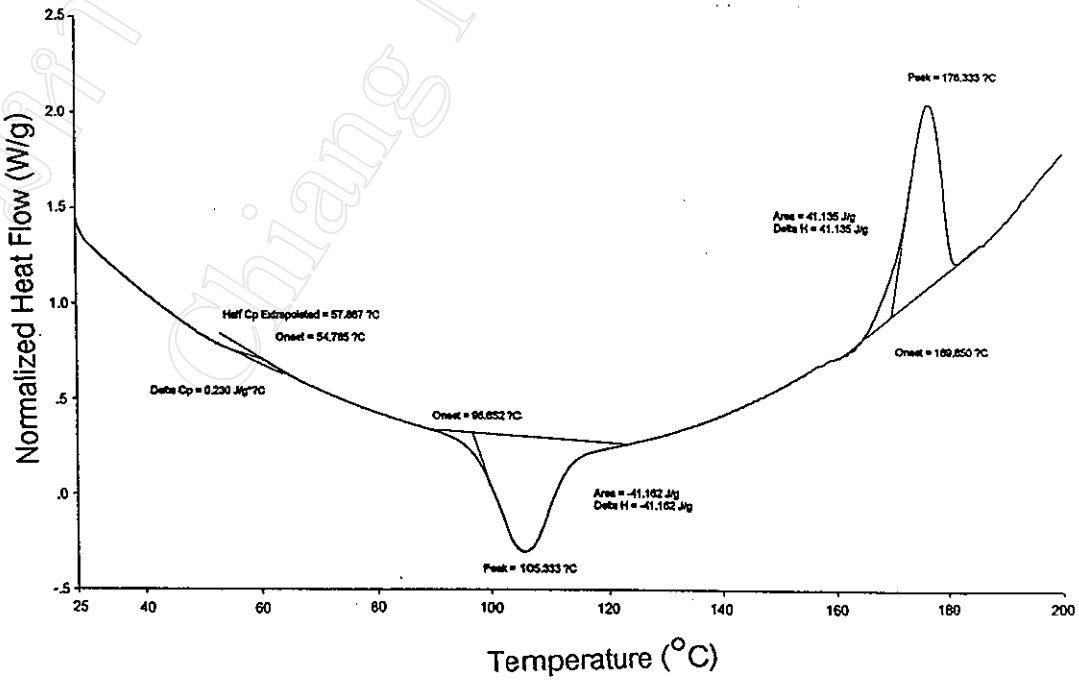

Figure 4.6 DSC thermogram of poly(L-lactide) synthesized at 140 °C for 72 hrs using SnOx as catalyst. (Sample size = 3.040 mg)

Table 4.6 DSC thermal transitions and melting parameters for poly(L-lactide) synthesized at 140 °C using $Sn(Oct)_2$ as catalyst.

Polymerization Time (hrs.)	DSC Thermal Transitions *			Melting Parameters *	
	T_g (°C)	T_c (°C)	T_m (°C)	ΔH_m (J/g)	Crystallinity (%)
1	45.1	77.0	150.0	41.7	44.5
2	56.4	88.7	165.3	45.8	48.9
3	54.0	97.3	168.0	46.7	49.8
6	54.4	100.3	174.3	45.0	48.0
12	55.6	105.3	176.0	45.2	48.2
18	55.7	98.3	175.7	52.2	55.7
24	56.5	106.3	177.3	47.3	50.5
48	57.9	105.3	176.3	41.1	43.9
72	54.9	105.7	178.0	41.3	44.1

* values corrected to the nearest 0.1 °C or 0.1 J/g from those given on the DSC thermograms

Table 4.7 DSC thermal transitions and melting parameters for poly(L-lactide) synthesized at 180 °C using $Sn(Oct)_2$ as catalyst.

Polymerization Time (hrs.)	DSC Thermal Transitions *			Melting Parameters *	
	T_g (°C)	T_c (°C)	T_m (°C)	ΔH_m (J/g)	Crystallinity (%)
6	55.4	112.0	174.3	41.0	43.8
12	54.7	108.3	169.7	42.0	44.8
18	53.0	113.0	173.3	39.0	41.6
24	59.4	125.3	169.0	42.0	44.8
48	51.2	123.3	154.7	20.7	22.1

* values corrected to the nearest 0.1 °C or 0.1 J/g from those given on the DSC thermograms

Table 4.8 DSC thermal transitions and melting parameters for poly(L-lactide) synthesized at 140 °C using SnOx as catalyst.

Polymerization Time (hrs.)	DSC Thermal Transitions *			Melting Parameters *	
	T_g (°C)	T_c (°C)	T_m (°C)	ΔH_m (J/g)	Crystallinity (%)
1	-	-	-	-	-
2	-	-	-	-	-
3	-	-	-	-	-
6	-	-	-	-	-
12	52.0	95.0	166.7	40.8	43.5
18	43.8	84.0	143.7	39.9	42.6
24	49.5	99.0	168.0	29.6	31.6
48	51.9	94.7	165.7	39.5	42.2
72	57.5	100.3	173.7	36.1	38.5

* values corrected to the nearest 0.1 °C or 0.1 J/g from those given on the DSC thermograms

Generally, a polymer's thermal transition temperatures increase with molecular weight at the beginning up to a certain molecular weight level above which they then become approximately constant, as shown below.

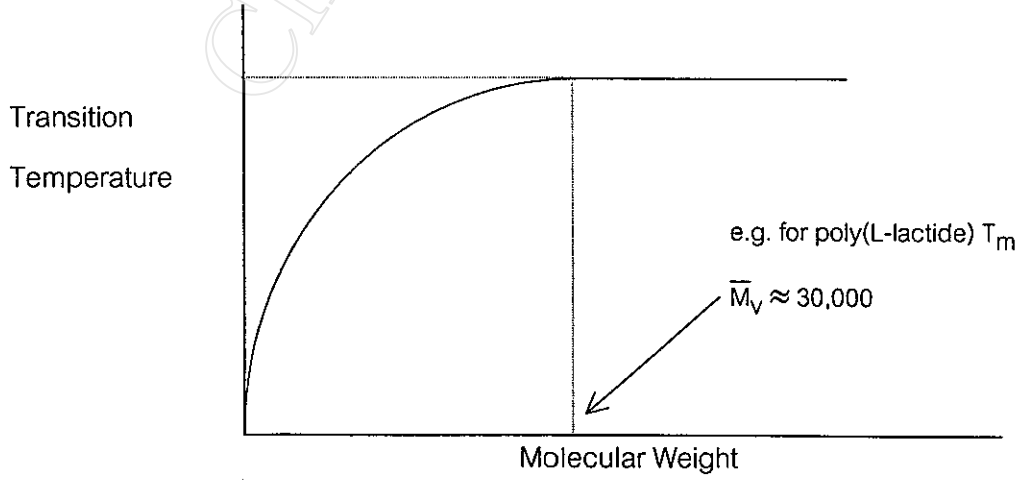

This molecular weight effect is most clearly seen when the T_m values in Table 4.6 are compared with the corresponding $\bar{M}_v$ values in Table 4.3. Together they indicate that, for poly(L-lactide), the molecular weight level at which T_m reaches its constant value is of the order of $\bar{M}_v \approx 3 \times 10^4$. Apart from this, the main conclusions to be drawn from these DSC results are that:

(1) there is not much difference in the ultimate (i.e., maximum) values of T_g, T_c and T_m obtained from the 3 experiments

(2) the values of T_g and T_m obtained compare favourably with the corresponding literature values [17] of 67 °C and 172-174 °C; the slightly lower T_g values from this work (< 60 °C) can be attributed to the fact that the samples were all nearly completely amorphous at the start of their DSC runs (lit. T_g = 67 °C is for a semi-crystalline sample)

(3) the polymer products are all semi-crystalline with similar % crystallinities as can be deduced from their similar ΔH_m values

The % crystallinities in Tables 4.6-4.8 were calculated from the ΔH_m values via the relationship:

$$\% \text{ crystallinity} = \frac{\Delta H_m}{\Delta H_m^*} \times 100$$

where ΔH_m^* is the theoretical heat of melting for a 100 % crystalline sample. In the case of poly(L-lactide), this value is obtained from the literature [30] as ΔH_m^* = 93.7 J/g. While the % crystallinities are similar, there are indications that:

(1) thermal degradation at the higher temperature of 180 °C decreases % crystallinity (see final sample in Table 4.7)

(2) using SnOx as catalyst (Table 4.8) gives a slightly lower % crystallinity than $Sn(Oct)_2$ (Table 4.6) under the same conditions

4.3 POLYMERIZATION KINETICS

4.3.1 Gravimetry

From the % conversions in Tables 4.3 – 4.5 obtained by gravimetry, the kinetic profiles in Figures 4.7, 4.9 and 4.11 are plotted as graphs of % conversion against time. These profiles can be considered alongside the corresponding viscosity-average molecular weight $\overline{M}_V$-time profiles in Figures 4.8, 4.10 and 4.12 respectively. The main points to note from these profiles are as follows:

1. <u>For the $Sn(Oct)_2$ – catalysed reaction at 140 °C,</u> the profile in Figure 4.7 shows that the main part of the reaction, up to > 90 % conversion, takes place during the first 12 hours. During this time, the $\overline{M}_V$ also increases rapidly up to about 4×10^4, as shown in Figure 4.8. This combination of high % conversion and high $\overline{M}_V$ after 12 hours coincides with the onset of solidification (Figure 4.7). Solidification occurs when the melting range of the polymer which is formed approaches the reaction temperature (140 °C), thus causing the system to gel. It is also interesting to note in Figures 4.7 and 4.8 that, even after the system has started to solidify, the % conversion and $\overline{M}_V$ still continue to increase as long as there is still some unreacted monomer remaining.

Even though molecular motion is severely restricted in the solid state, polymerization can still continue, albeit at a greatly reduced rate, due to the fact that the remaining monomer and catalyst are concentrated in the amorphous (i.e., non-crystalline) regions of the polymer matrix [31]. Consequently, the monomer is still able to diffuse to the active catalyst sites, provided that the reaction temperature (140 °C) is above the polymer's glass transition temperature (T_g of PLL ≈ 67 °C). It is this

molecular diffusion which enables the reaction to continue to proceed towards 100 % conversion.

2. For the $Sn(Oct)_2$–catalysed reaction at 180 °C, the reaction profile in Figure 4.9 confirms the expected increase in the rate at this higher temperature. The time to maximum conversion is considerably reduced. However, this increase in rate is also accompanied by a decrease in $\overline{M}_V$ at long reaction times (Figure 4.10), indicative of thermal degradation of the polymer.

Thermal degradation of PLL at high temperatures may occur by either intra- or intermolecular transesterification. The former decreases the average molecular weight while the latter merely broadens the molecular weight distribution [11, 32]. These 2 transesterification mechanisms are compared below.

(a) Intramolecular transesterification via back–bitting

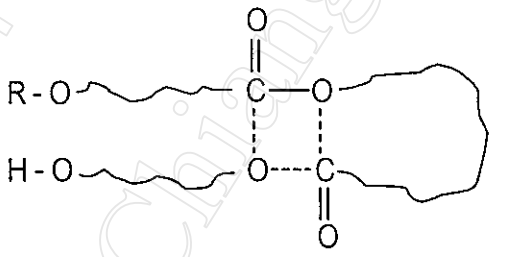

1 molecule

mol. wt. reduction

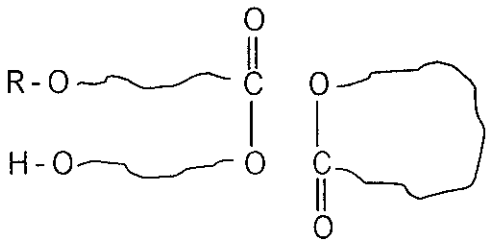

2 molecules

(b) Intermolecular transesterification

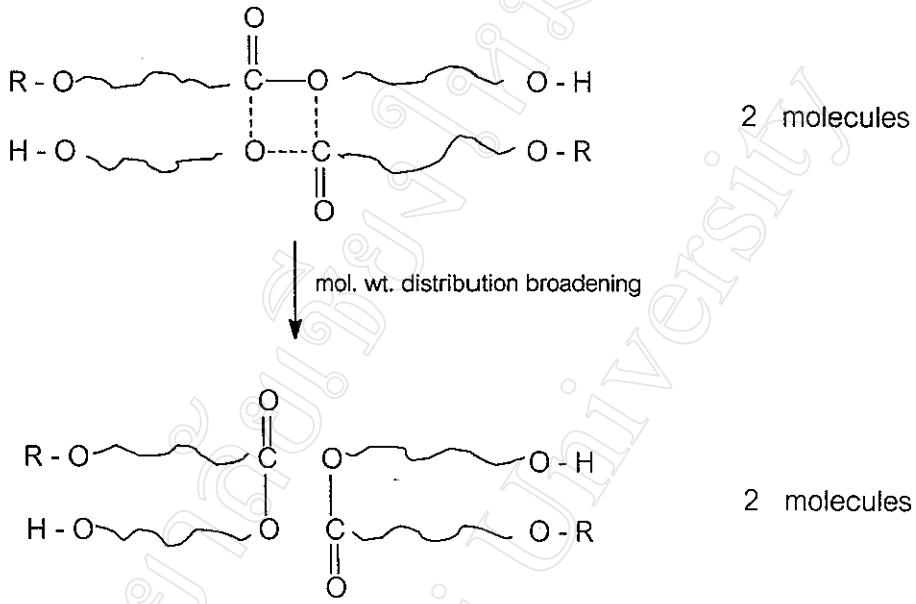

3. For the SnOx-catalysed reaction at 140 °C, the reaction profile in Figure 4.11 clearing shows that the reaction is much slower than the $Sn(Oct)_2$–catalysed reaction at the same temperature. This demonstrates the effect of catalyst structure on the kinetics of the reaction. When used in conjunction with an alcohol initiator, the active site in these organotin compounds for coordination with the L-lactide monomer is generally accepted to be the Sn-O bond. In $Sn(Oct)_2$, the Sn-O bond is unconstrained within the linear molecule. However, in SnOx, the Sn-O bond is constrained within a 5-membered ring. This suggests that the constraints of the ring somehow decrease the catalytic activity of SnOx relative to $Sn(Oct)_2$. Despite this, the final % conversion and $\bar{M}_v$ after 72 hours for SnOx is comparable to those for $Sn(Oct)_2$ after 12 hours.

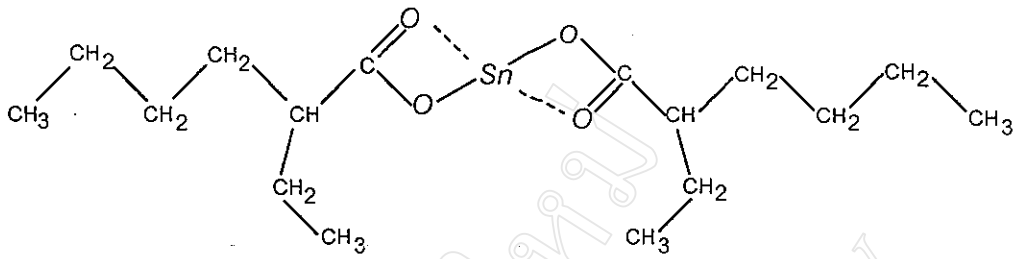

$Sn(Oct)_2$

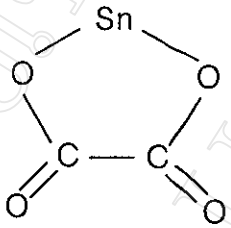

SnOx

4. General Observation

It should also be mentioned here that a 0 % conversion (except at time t = 0) does not necessarily mean that no reaction had occurred. This highlights the main disadvantage of the gravimetric method. Only if the polymer molecular weight is high enough will the polymer be able to precipitate from solution as a solid which can be filtered off. Consequently, in the initial stages of the reaction when the molecular weight is still very low, it is quite possible that no solid polymer will be recoverable even though the reaction has already started. This problem will then persist as the reaction proceeds for as long as the lowest molecular weight fraction is unable to precipitate. However, as the molecular weight average and distribution both shift towards a higher molecular weight range, this problem decreases until the % recovery, and hence the calculated % conversion, is near-quantitative towards the end of the reaction.

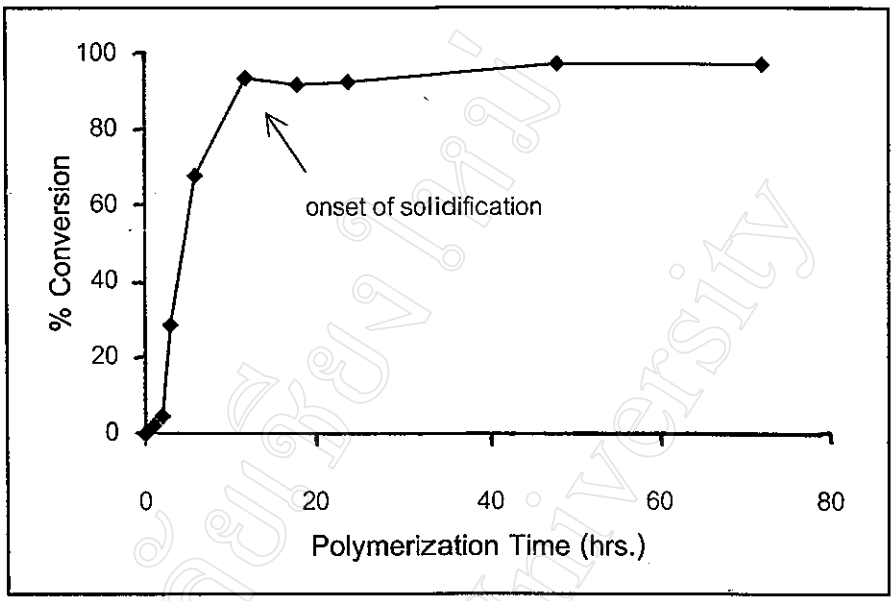

Figure 4.7 L-Lactide conversion-time profile using $Sn(Oct)_2$ as catalyst at 140 °C.

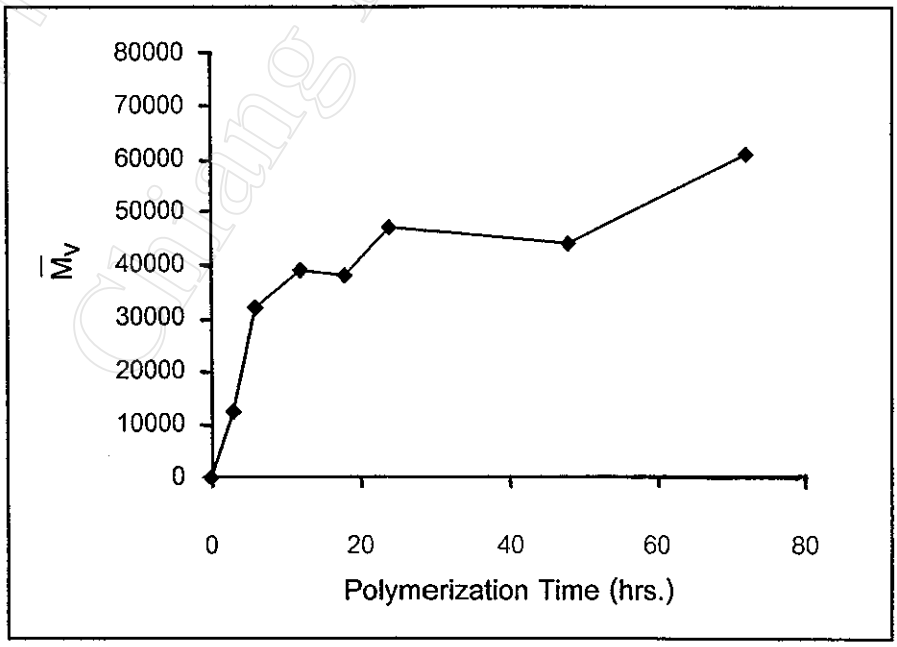

Figure 4.8 L-Lactide $\bar{M}_V$-time profile using $Sn(Oct)_2$ as catalyst at 140 °C.

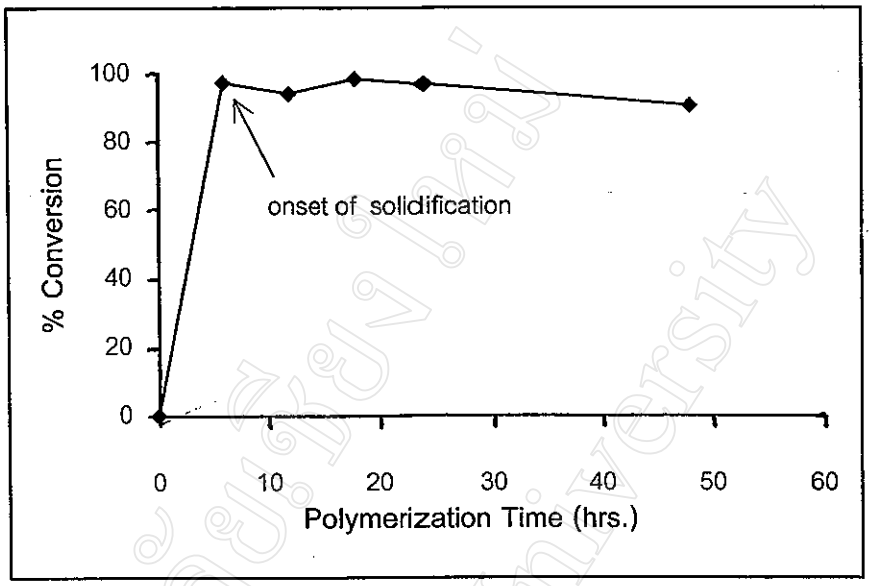

Figure 4.9 L-Lactide conversion-time profile using $Sn(Oct)_2$ as catalyst at 180 °C.

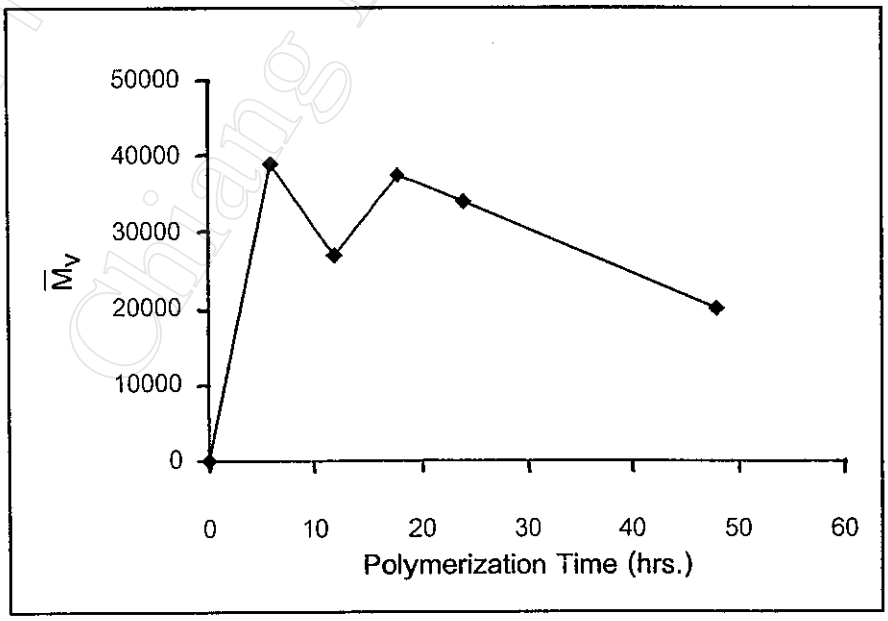

Figure 4.10 L-Lactide $\bar{M}_V$-time profile using $Sn(Oct)_2$ as catalyst at 180 °C.

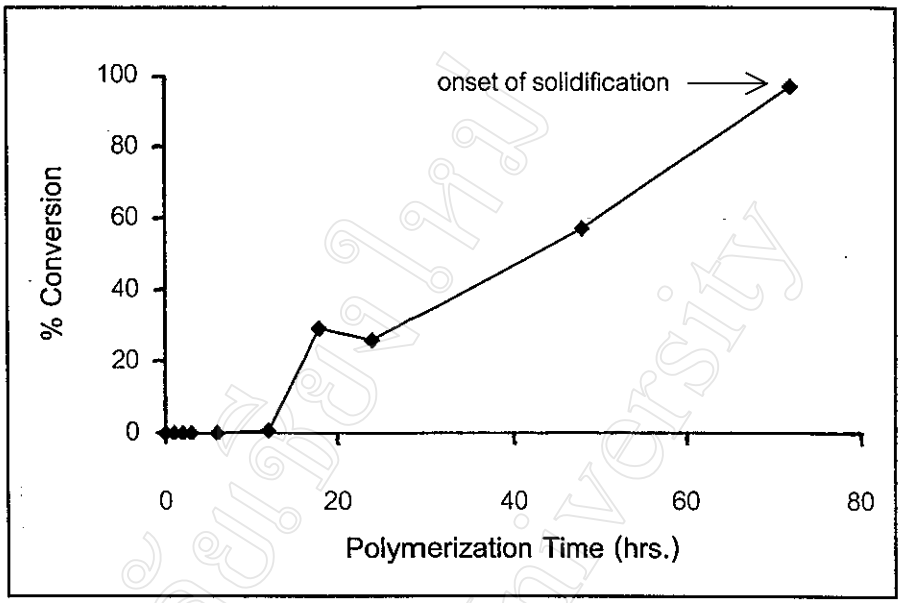

Figure 4.11 L-Lactide conversion-time profile using SnOx as catalyst at 140 °C.

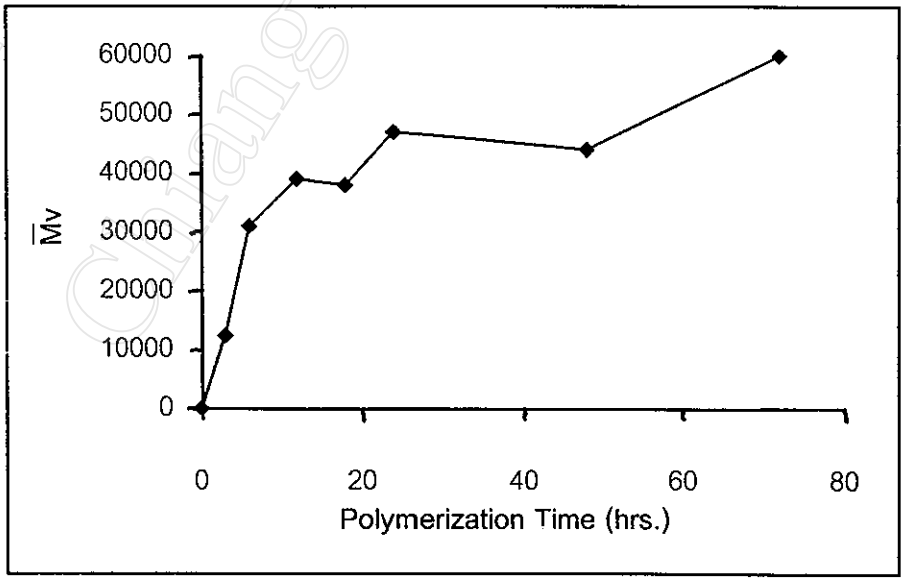

Figure 4.12 L-Lactide $\bar{M}_V$-time profile using SnOx as catalyst at 140 °C.

4.3.2 Infrared Spectroscopy (FT-IR)

4.3.2.1 Structural Characterisation

The Fourier-transform (FT-IR) infrared spectra of the highest molecular weight purified poly(L-lactide) products obtained using $Sn(Oct)_2$ as catalyst at 140 °C and 180 °C and SnOx as catalyst at 140 °C are shown in Figures 4.13, 4.14 and 4.15 respectively. They can be compared with the reference IR spectrum of poly(L-lactide) in Figure 4.16 (a). The major vibrational peak assignments are listed in Table 4.9 and are seen to be consistent with the polymer's chemical structure:

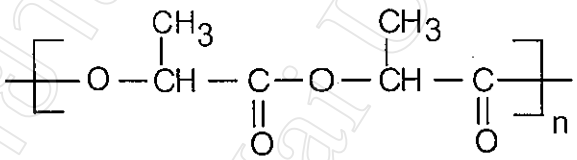

The spectra were obtained from solid films cast from solution in chloroform onto sodium chloride discs.

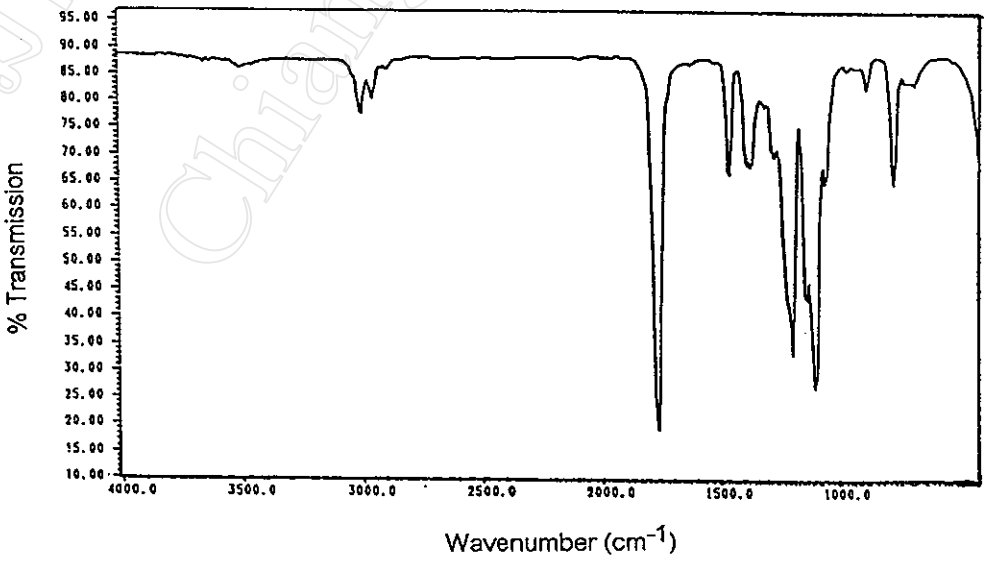

Figure 4.13 FT-IR spectrum of the purified poly(L-lactide) synthesized at 140 °C for 72 hrs using $Sn(Oct)_2$ as catalyst. (PLL 1)

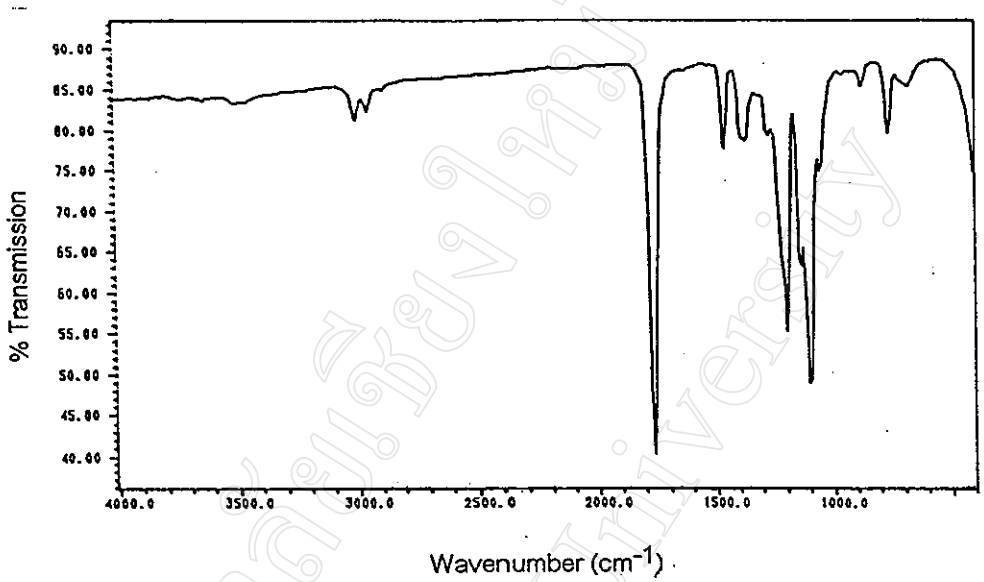

Figure 4.14 FT-IR spectrum of the purified poly(L-lactide) synthesized at 180 ^{o}C for 6 hrs $Sn(Oct)_2$ as catalyst. (PLL 2)

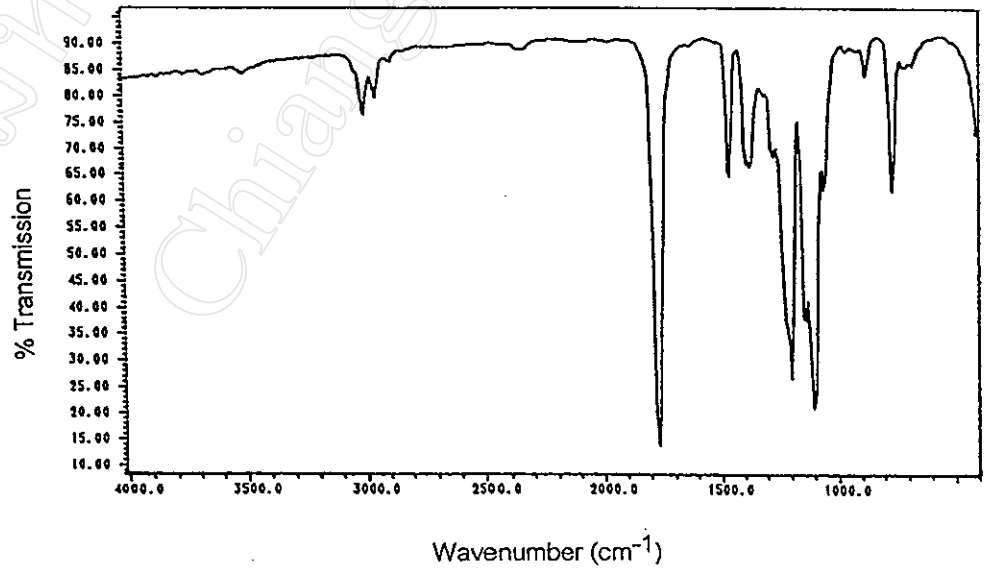

Figure 4.15 FT-IR spectrum of the purified poly(L-lactide) synthesized at 140 ^{o}C for 72 hrs using SnOx as catalyst. (PLL 3)

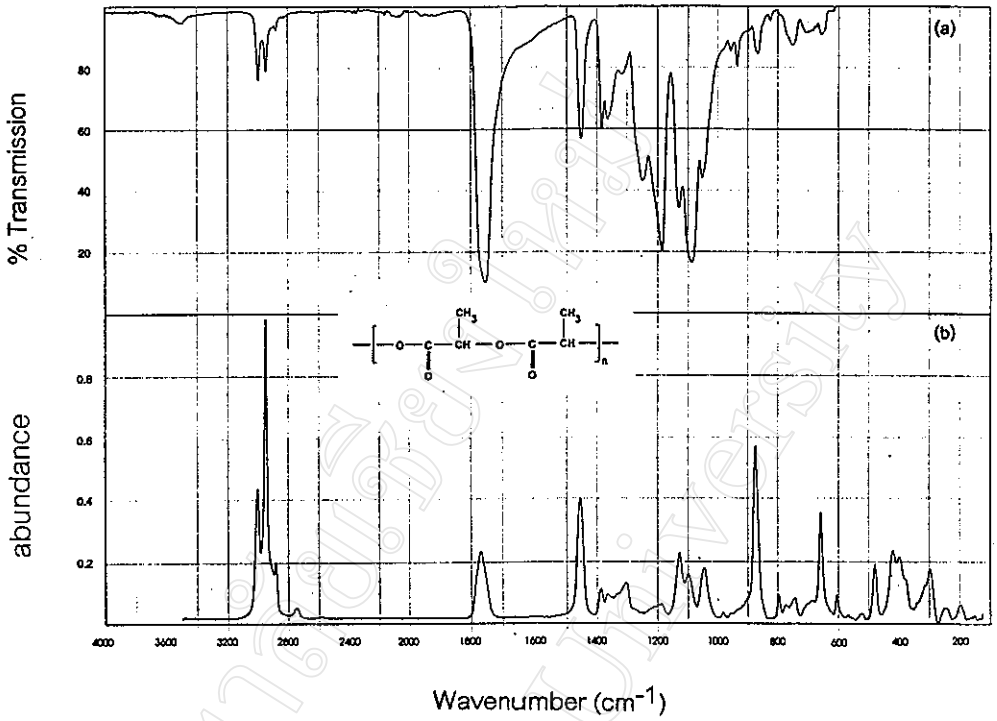

Figure 4.16 Reference Fourier-transform (FT) vibrational spectra of poly(L-lactide) [28].

(a) FT-IR spectrum

(b) FT-Raman spectrum

Table 4.9 Main vibrational assignments in the poly(L-lactide) FT-IR spectra.

VIBRATIONAL ASSIGNMENT	WAVENUMBER (cm^{-1})			
	Reference	PLL 1	PLL 2	PLL 3
O – H stretching*	3600-3400	3600-3400	3600-3400	3600-3400
C – H stretching	2900-2850	3100-2900	3100-2900	3100-2900
C = O stretching	1750	1775	1775	1775
C – H bending	1450	1475	1400	1400
C – O stretching, acyl-oxygen	1190	1200	1200	1200
C – O stretching, alkyl-oxygen	1090	1100	1100	1100

* very weak absorbances arising from OH end-groups in the polymer

4.3.2.2 Kinetic Studies

Following on from the previous gravimetric method, with its known advantages and disadvantages, this FT-IR method offers an interesting comparison. It is based on the disappearance of monomer peaks and the appearance of polymer peaks in the spectrum as the reaction proceeds. A recent literature report [11] described a method by which 2 absorption bands in the FT-IR spectrum of polymerizing L-lactide (LL) could be used to calculate the % conversion at any time. These 2 bands are those at 1383 cm^{-1}, a C-H bending band shared by both the monomer and the polymer (LL + PLL), and at 935 cm^{-1}, a C-H bending band specific to the monomer only (LL). A calibration plot of the [PLL] / [LL] molar ratio against the A_{1383}/A_{935} peak absorbance ratio was established. The % conversion was then calculated from:

$$\% \text{ Conversion} = \frac{[PLL]}{[LL]+[PLL]} \times 100$$

$$= \frac{100}{([LL]/[PLL]+1)}$$

where

$$[PLL]/[LL] = -12.27 + 31.56(A_{1383}/A_{935}) - 26.76(A_{1383}/A_{935})^2 + 10.43(A_{1383}/A_{935})^3 - 1.81(A_{1383}/A_{935})^4 + 0.12(A_{1383}/A_{935})^5$$

Two examples of the FT-IR spectra (absorbance mode) obtained in this work are shown in Figures 4.17 and 4.18. They were obtained from thin films of the whole polymerizate cast from solution in chloroform directly onto sodium chloride discs. The two spectra serve to show (a) how the ratio of the absorbances of the 2 peaks at 1383 cm^{-1} and 935 cm^{-1} varies as the reaction proceeds and (b) how the tangent lines to the peaks are constructed in order to measure their absorbances. A sample calculation showing how the absorbance ratio A_{1383} / A_{935} is converted into a % conversion is given below:

Sample Calculation

From the spectrum in Figure 4.17 for the PLL / SnOx / 140 °C / 1 hr sample:

A_{1383} = 0.42 scale divisions

A_{935} = 0.45 scale divisions

A_{1383} / A_{935} = 0.93

[PLL] / [LL] = $-12.27 + 31.56(0.93) - 26.76(0.93)^2 + 10.43(0.93)^3 - 1.81(0.93)^4 + 0.12(0.93)^5$

= 1.06

Thus, [LL] / [PLL] = 1 / 1.06 = 0.94

Hence, $$\% \text{ Conversion} = \frac{100}{0.94 + 1} \%$$

% Conversion = 51.5 %

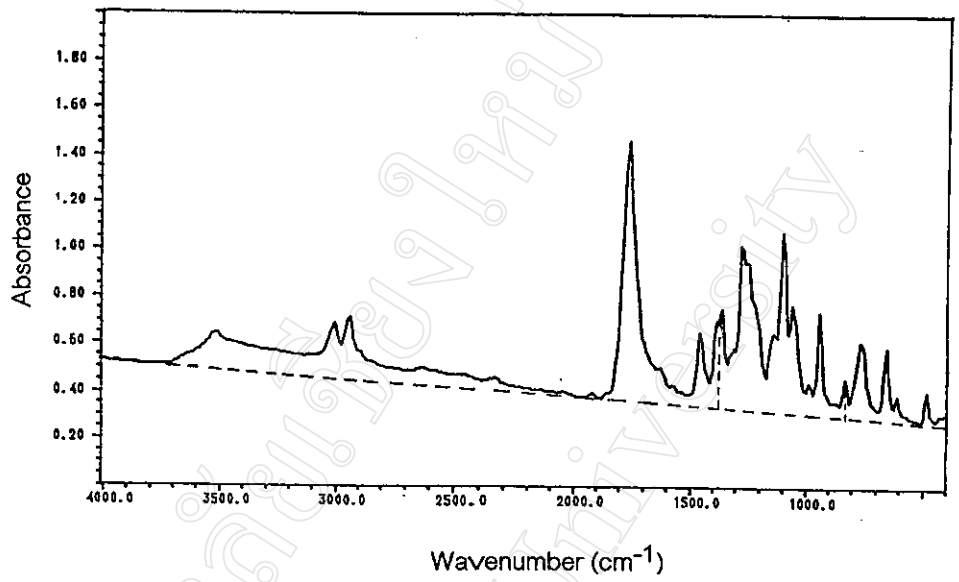

Figure 4.17 FT-IR spectrum (absorbance mode) of the L-lactide/poly(L-lactide) polymerisate after 1 hr at 140 °C using SnOx as catalyst.

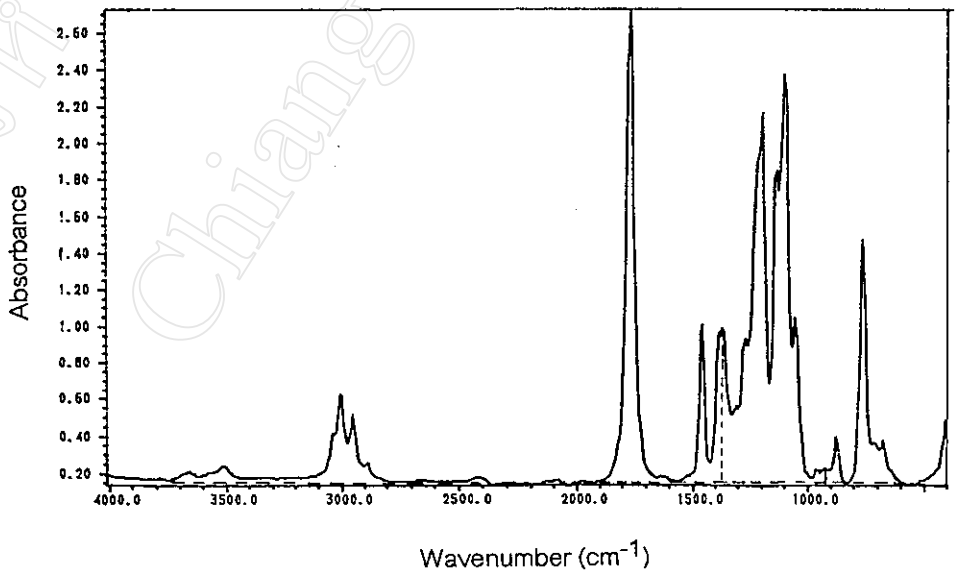

Figure 4.18 FT-IR spectrum (absorbance mode) of the L-lactide/poly(L-lactide) polymerisate after 48 hrs at 140 °C using SnOx as catalyst.

Table 4.10 Values of the absorbance ratios and % conversions from the FT-IR absorbance spectra for poly(L-lactide) synthesized at 140 °C using $Sn(Oct)_2$ and SnOx as catalysts.

Polymerization Time (hrs)	$Sn(Oct)_2$		SnOx	
	Absorbance Ratio *	Conversion %	Absorbance Ratio *	Conversion %
1	0.84	40.8	0.93	51.5
2	1.04	57.6	0.93	51.5
3	17.83**	100.0	1.39	58.2
6	6.43	98.8	1.81	65.9
12	7.29	99.5	2.46	76.3
18	6.33	98.7	3.33	88.6
24	7.29	99.5	6.43	98.8
48	6.33	98.7	14.17	100.0
72	8.00	99.7	14.17	100.0

* Absorbance Ratio = A_{1383} / A_{935}

** spurious result

The absorbance ratios and calculated % conversions for the $Sn(Oct)_2$ and SnOx-catalysed polymerizations at 140 °C are given in Table 4.10 and plotted against time in Figure 4.19. The corresponding $\bar{M}_V$-time profiles from dilute-solution viscometry are also shown again for comparison in Figure 4.20. For calculating the absorbance ratio, it is first necessary to construct a baseline to the spectrum. As shown in Figures 4.17 and 4.18, this is most conveniently done by drawing a line through the absorbance minima. The absorbance of any given peak is then proportional to the length of a line (in scale divisions) drawn from the baseline to the peak maximum.

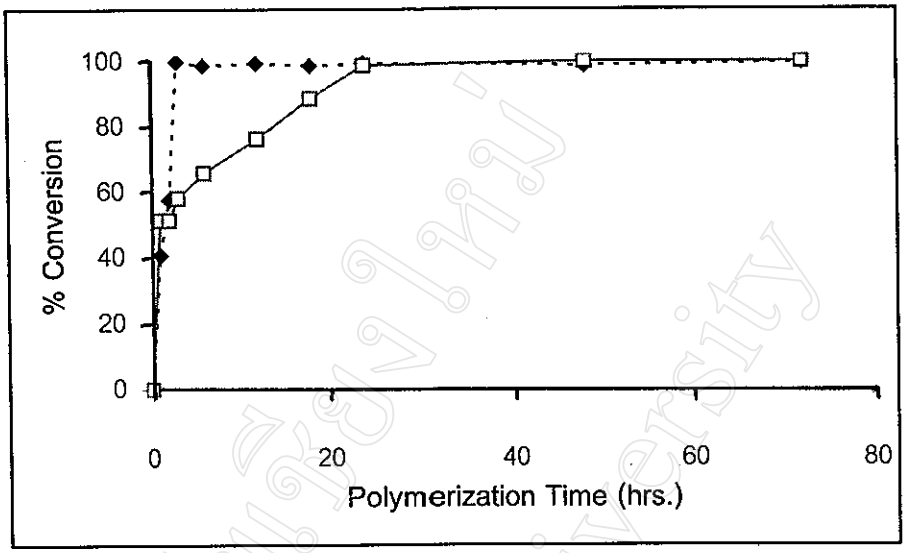

Figure 4.19 Comparison of the % conversion-time profiles using $Sn(Oct)_2$ and SnOx as catalysts at 140 °C, as obtained from FT-IR absorbance data.

♦ $Sn(Oct)_2$ □ SnOx

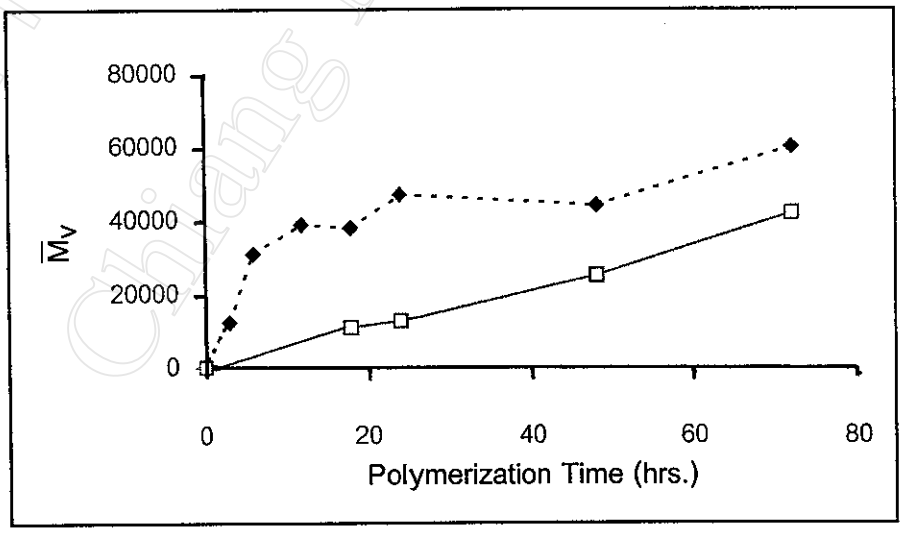

Figure 4.20 Comparison of the $\bar{M}_V$-time profiles using $Sn(Oct)_2$ and SnOx as catalysts at 140 °C, as obtained from dilute-solution viscometry.

♦ $Sn(Oct)_2$ □ SnOx

From the % conversion-time profiles in Figure 4.19, the rate of polymerization using $Sn(Oct)_2$ as catalyst is again seen to be higher than that using SnOx, consistent with the previous gravimetric results. The fact that these 2 quite different methods, FT-IR and gravimetry, give rise to this same conclusion is strong evidence in its support. However, when the FT-IR and gravimetry results are compared side by side in Figures 4.21 and 4.22, we can see that there are also differences too, most notably:

1. In all cases, the % conversion obtained from FT-IR is higher than that from gravimetry. This is especially true during the initial stages of the reaction when the molecular weight ($\overline{M}_V$) of the polymer formed is still low (Figure 4.20). However, as the % conversion and $\overline{M}_V$ increase, the FT-IR and gravimetry profiles in Figure 4.21 and 4.22 converge. Therefore, these FT-IR results further reinforce the point made earlier about the main disadvantage of the gravimetry method. Even though it is an absolute method, gravimetry is insensitive during the initial part of the reaction when the polymer molecular weight is not high enough for the polymer to precipitate completely from solution. Consequently, the % conversion obtained is less than reality. In contrast, the FT-IR method does not suffer from this problem. As soon as the L-lactide monomer reacts, even to form low molecular weight oligomers ($\overline{DP}_n$ < 10), the peaks at 1383 and 935 cm^{-1} change accordingly. Although this would seem to be a considerable advantage of the FT-IR method, it must be remembered that it is not an absolute method since it depends on the accuracy of the % conversion-absorbance ratio calibration.

2. The difference in the FT-IR and gravimetry profiles for the SnOx-catalyzed reaction in Figure 4.22 emphasizes how cautious we must be when interpreting the results from a given method. Different methods can give quite different results and we should be aware of their respective strengths and weaknesses before drawing any firm conclusions

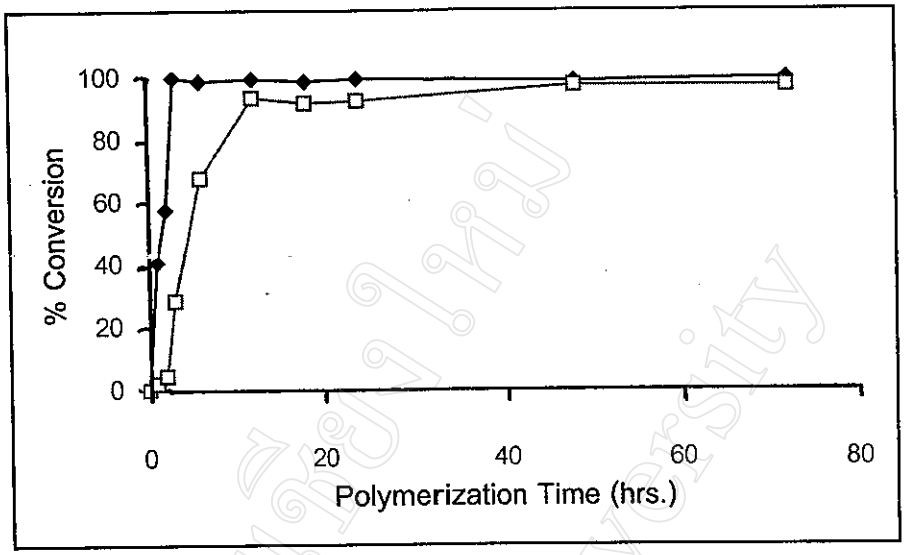

Figure 4.21 Comparison of the % conversion-time profiles from FT-IR and gravimetric data for the polymerization of L-lactide using $Sn(Oct)_2$ as catalyst at 140 °C.

♦ FT-IR □ gravimetry

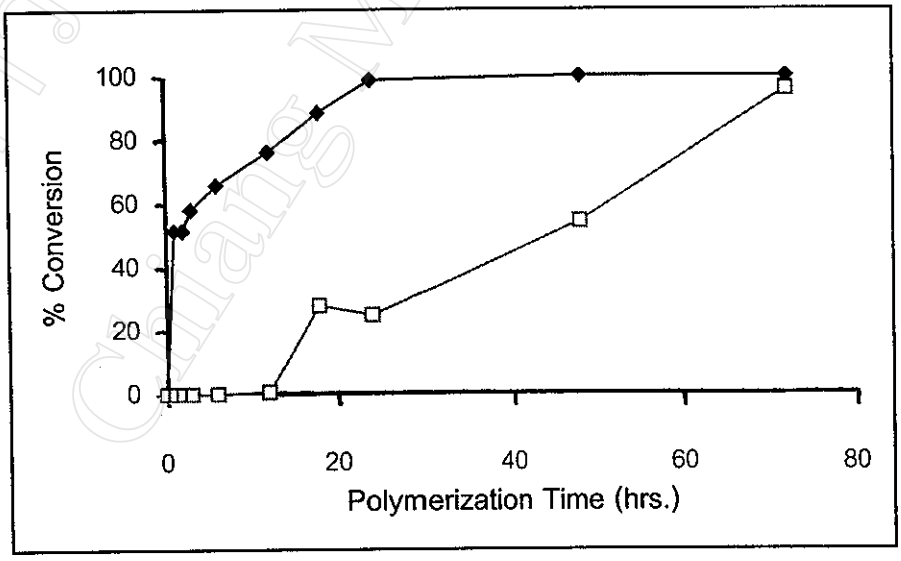

Figure 4.22 Comparison of the % conversion-time profiles from FT-IR and gravimetric data for the polymerization of L-lactide using SnOx as catalyst at 140 °C.

♦ FT-IR □ gravimetry

4.3.3 Proton Nuclear Magnetic Resonance Spectroscopy (^{1}H-NMR)

4.3.3.1 Structural Characterisation

Following on from gravimetry and FT-IR, the third method which was investigated in this work as a means of following the kinetics of L-lactide polymerization was proton nuclear magnetic resonance (^{1}H-NMR) spectroscopy. As in FT-IR previously, this ^{1}H-NMR method is also based on the principle that, as a particular peak in the monomer spectrum decreases with conversion, so the corresponding peak in the polymer spectrum increases. In a recent literature report [11], it was suggested that the methine (C-H) protons could be used for this purpose since their chemical shift (peak centre) changes slightly from δ = 5.02 ppm in L-lactide monomer to δ = 5.16 ppm in poly(L-lactide) polymer.

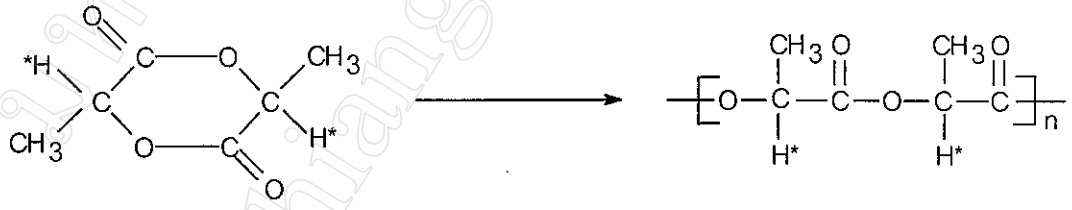

L-Lactide poly(L-lactide)

* $\delta_{C\text{-}H}$ = 5.02 ppm * $\delta_{C\text{-}H}$ = 5.16 ppm

This slight change in chemical shift can be seen by comparing the ^{1}H-NMR spectra of the L-lactide (recrystallized) and poly(L-lactide) (purified) prepared in this work. The spectra are shown in Figures 4.23 and 4.24 respectively and the various peaks assigned in Table 4.11. It can be seen that the quartet resonance due to the methine C-H protons in L-lactide, centred at δ = 5.09 ppm (Figure 4.23), shifts to δ = 5.18 ppm (Figure 4.24) in poly(L-lactide). This represents a shift of 0.09 ppm. In comparison, the doublet resonance due to the methyl CH_3 protons changes from δ = 1.64 ppm in the monomer to δ = 1.58 ppm in the polymer, a shift of only 0.06 ppm.

The use of ^{1}H-NMR in the study of polymerization kinetics is made possible by the fact that the area under a given peak is directly proportional to the number of protons which are responsible for the peak. Therefore, via peak area integration, it is possible to calculate the % conversion in a polymerization mixture provided that corresponding monomer and polymer peaks are sufficiently well separated for their peak area integrations not to overlap.

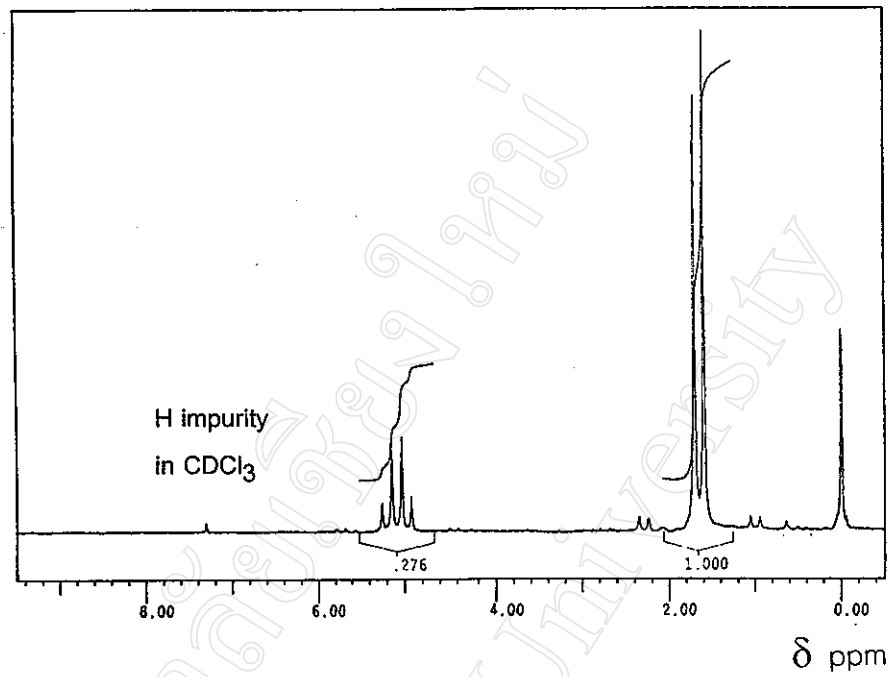

Figure 4.23 60 MHz ^{1}H-NMR spectrum of L-lactide (recrystallized) in $CDCl_3$ as solvent at 21 ^{o}C.

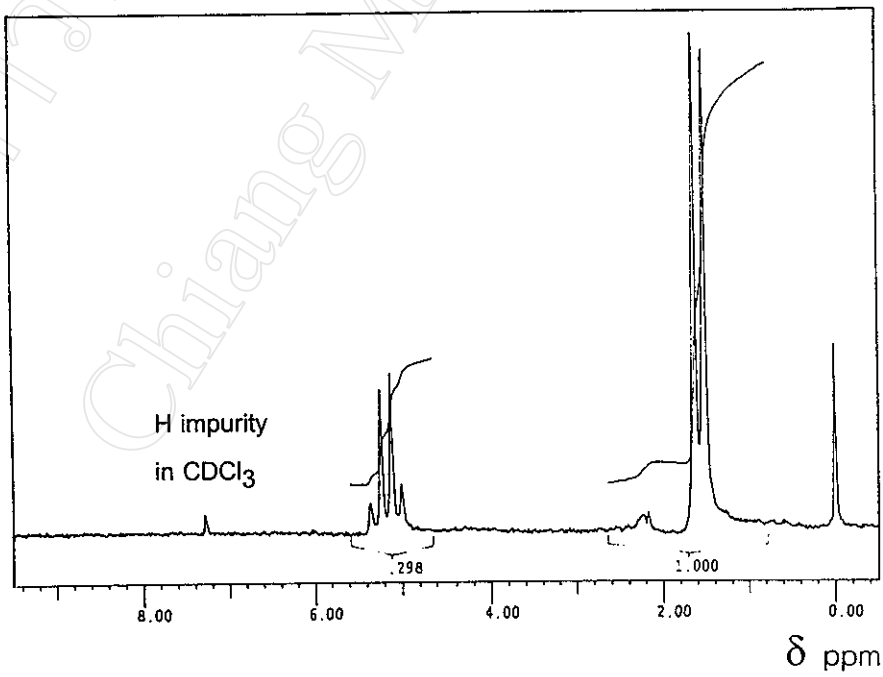

Figure 4.24 60 MHz ^{1}H-NMR spectrum of poly(L-lactide) (purified) in $CDCl_3$ as solvent at 21 ^{o}C.

(Polymer synthesized using $Sn(Oct)_2$ as catalyst at 140 ^{o}C for 72 hrs.)

Table 4.11 Interpretation of the ^{1}H-NMR spectra of the L-lactide (recrystallized) and poly(L-lactide) (purified) samples shown in Figure 4.23 and 4.24 respectively.

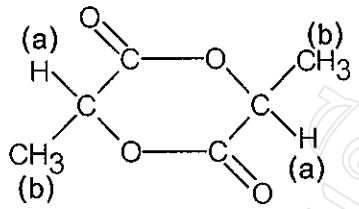

L-lactide

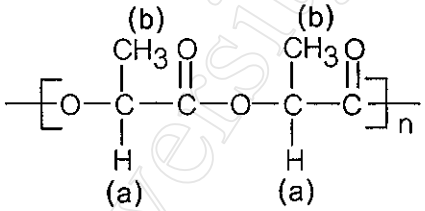

poly(L-lactide)

Proton Assignment	Peak Multiplicity	Chemical Shift *, δ (ppm)	
		L-lactide	Poly(L-lactide)
a	Quartet	5.09	5.18
b	Doublet	1.64	1.58

* taken as the peak centre of each quartet/doublet

4.3.3.2 Kinetic Studies

The particular NMR instrument used in this work was a 60 MHz Hitachi R-1500 ^{1}H-NMR Spectrometer operating at room temperature. Unfortunately, the instrument was out of order for some time during the period that it was needed in this project with the result that only 3 polymerizate sample analyses were possible. These 3 samples were the first 3 samples (times = 1, 2 and 3 hrs.) of the $Sn(Oct)_2$-catalyzed polymerization at 140 °C. Their ^{1}H-NMR spectra are shown in Figures 4.25-4.27 respectively. Even though the results in this NMR section of the work are incomplete, they still allow for some interesting observations to be made regarding the nature of the reaction and for a preliminary evaluation of the usefulness of this NMR method for kinetic studies.

The peak assignments for the 3 NMR spectra in Figures 4.25-4.27 are given in Table 4.12. The most notable features are:

(1) A new quartet resonance appears at δ 4.1-4.7 which can be assigned to the methine C-H proton in the polymer at the hydroxyl-terminated chain end. Indeed, it is the proximity of the OH end-group which enables the peak to be distinguished from the main chain methine C-H protons at δ 4.8-5.5. This new peak is very prominent in Figure 4.25 (time = 1 hr.) and Figure 4.26 (time = 2 hrs.) which indicates that the chain end concentration is still very high (i.e., the polymer molecular weight is still very low) after 2 hrs. This is consistent with the previous gravimetry results (Table 4.3) which gave very low (< 5%) conversion during the first 2 hours of the $Sn(Oct)_2$-catalysed polymerization at 140 °C. However, this chain end methine C-H resonance is much reduced in Figure 4.27 (time = 3 hrs.) which indicates that a significant increase in molecular weight

took place during the 3rd hour of the reaction, consistent with the increase in % conversion to nearly 30 % (Table 4.3)

(2) In contrast to the clear separation of the chain end methine C-H resonance, the methine C-H resonance belonging to the polymer main chain units and to the residual monomer still overlap in the δ 4.8-5.5 range of the spectra. Therefore, it is impossible to calculate the % conversion from the peak area integrations in Figures 4.25-4.27. The only way that this might be achieved is with a much higher resolution instrument (i.e., higher magnetic field frequency > 100 MHz) combined with scale expansion. As mentioned in the previous section, the difference between the chemical shifts of the monomer and polymer methine C-H peak centres is only about 0.1 ppm. Such a small difference makes it very difficult to distinguish between the two. In order to calculate the % conversion, the two peaks need to be well separated.

Thus, this NMR method has been unsuccessful in this work for studying the reaction profile. It has, however, shown itself to be a potentially useful technique for showing how the end-unit concentration decreases with time during the initial part of the reaction. This is of mechanistic interest since it seems to be a characteristic of this alcohol-initiated coordination-insertion type of reaction that there is a sort of "induction period" at the beginning during which the molecular weight increases more slowly than expected.

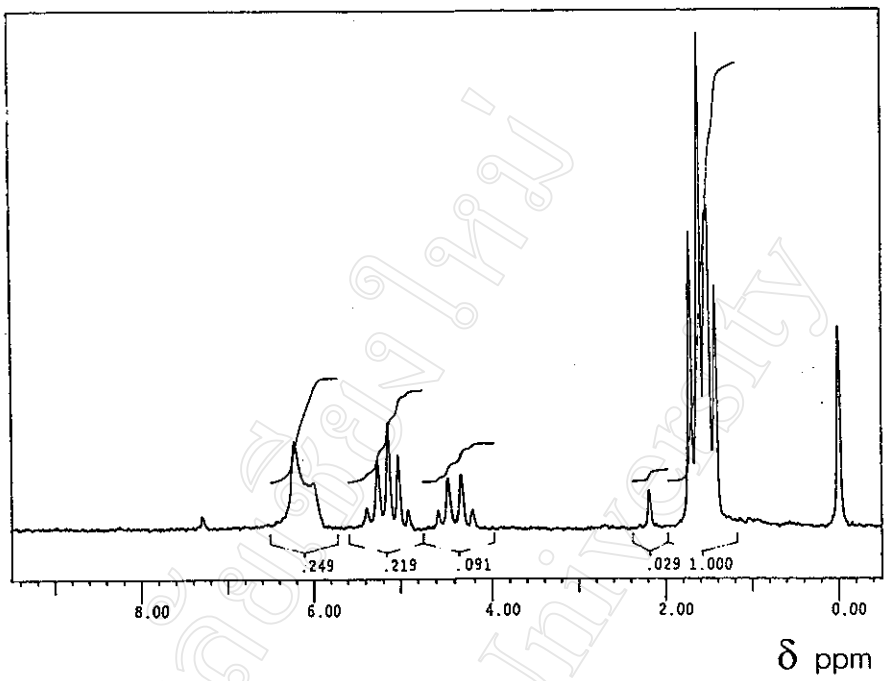

Figure 4.25 60 MHz ^{1}H-NMR spectrum of the polymerizate from the L-lactide polymerization using $Sn(Oct)_2$ as catalyst at 140 ^{o}C for 1 hr.

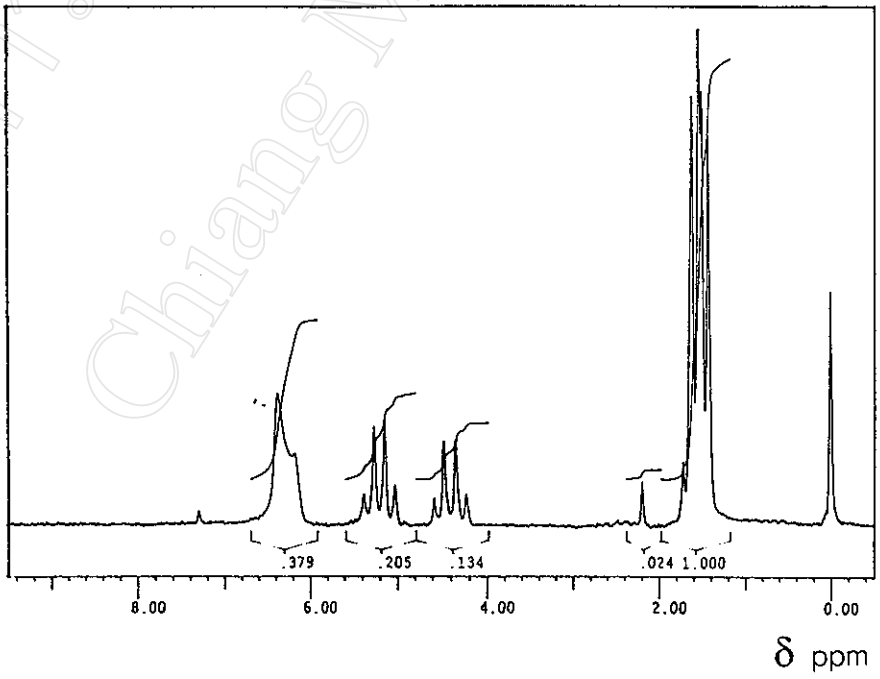

Figure 4.26 60 MHz ^{1}H-NMR spectrum of the polymerizate from the L-lactide polymerization using $Sn(Oct)_2$ as catalyst at 140 ^{o}C for 2 hr.

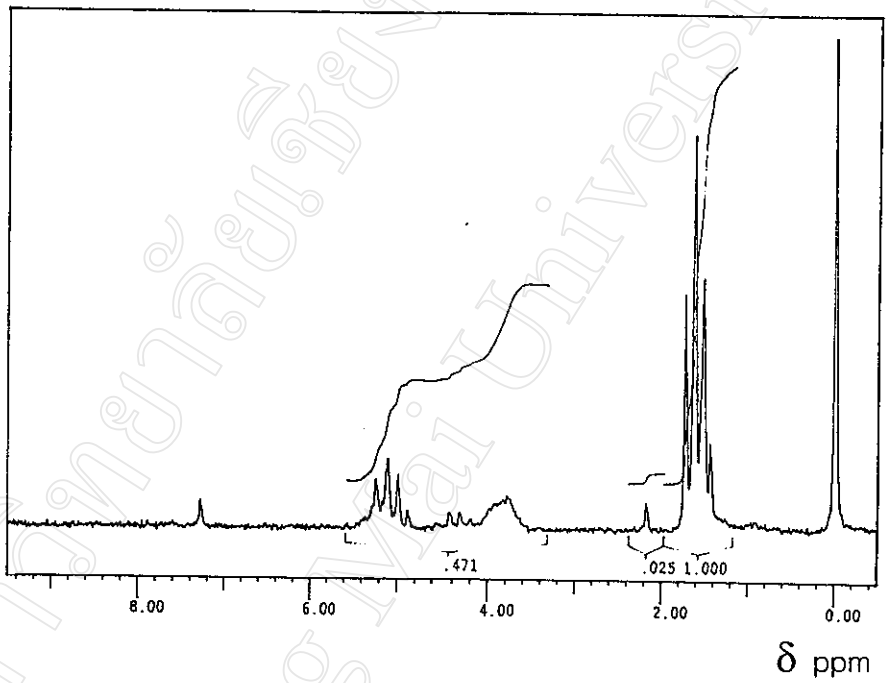

Figure 4.27 60 MHz ^{1}H-NMR spectrum of the polymerizate from the L-lactide polymerization using $Sn(Oct)_2$ as catalyst at 140 ^{o}C for 3 hr.

Table 4.12 Interpretation of the ^{1}H-NMR spectra of the polymerizates shown in Figures 4.25-4.27.

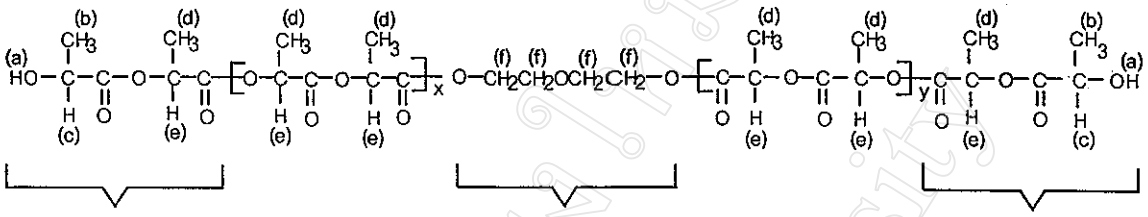

hydroxyl-terminated chain end unit | from DEG initiator | hydroxyl-terminated chain end unit

poly(L-lactide)

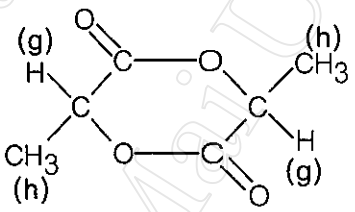

L-Lactide

Proton Assignment	Chemical Shift *, δ (ppm)		
	Figure 4.25	Figure 4.26	Figure 4.27
a	5.9 – 6.5	6.0 – 6.7	3.5 – 4.1
b, d, h **	1.3 – 1.9	1.3 – 1.9	1.3 – 1.9
c	4.1 – 4.6	4.1 – 4.7	4.1 – 4.7
e, g **	4.8 – 5.5	4.8 – 5.5	4.8 – 5.5
f	not observed	not observed	not observed

* given as a range covering the whole peak

* * overlapping peaks